MFR PAPER 1147

Fine Structure of *Minchinia* sp. (Haplosporida) Sporulation in the Mud Crab, *Panopeus herbstii*

FRANK O. PERKINS

ABSTRACT—Morphogenetic changes which accompany sporulation of Minchinia *sp. in the mud crab (*Panopeus herbstii*) are described. Small (4-19 μm diameter) plasmodia, the precursor cells for the sporulation sequence, increase in size and numbers of nuclei per cell to form sporonts with a delimiting wall. Since widely divergent nuclear sizes (2.3-5.9 μm diameter) and paired small nuclei (<3 μm diameter) were observed in sporonts, it is suggested that karyogamy occurs followed by meiosis. Evidence for meiosis is the observation of synaptonemal-like complexes and polycomplex-like structures in sporont nuclei. Sporonts cleave into uninucleate sporoblasts following one of two pathways. In the presumably "normal" sequence, a cytoplasmic syncytium is formed followed by cleavage into uninucleate sporoblasts. In the other, sporont protoplasm is asynchronously "carved" into uni- or binucleate sporoblasts or sporoplasms as a result of delimitation at the surface and internally. Since aberrant spore formation was commonly observed in the latter type of sporont, its cleavage patterns are considered to be anomalous. A sporoplasm is then delimited in each sporoblast and spore maturation follows. Haplosporosomes were observed in plasmodia and spores, but not in intermediate cell stages. Mitotic apparati appear to be persistent through interphase in plasmodia and sporonts and consist of two spindle pole bodies connected by a bundle of microtubules.*

INTRODUCTION

A species of *Minchinia*, parasitizing the mud crab, *Panopeus herbstii*, was obtained from the York River, Virginia estuary. Collection sites were intertidal and subtidal in the salinity range of about 6 to 22‰. The haplosporidan closely resembles *Minchinia louisiana* (Sprague, 1963) except that spores of the Louisiana species average 12.1 μm long by 8.4 μm wide whereas those of the Virginia species average 9.6 × 8.1 μm (N = 30; range = 9.0-10.0 × 7.5-9.0 μm). Therefore, since spore size is considered to be an important species characteristic used in haplosporidan taxonomy (see for examples: Couch, 1967; Sprague, 1963; Wood and Andrews, 1962), the present sporozoan will be considered as *Minchinia* sp.

The ultrastructure of spore formation in other closely related Haplosporida has been studied by Perkins (1968; 1969; 1971) and Ormières et al. (1973). Spore fine structure of several species has been described by Ormières and de Puytorac (1968) and Rosenfield et al. (1969). One of the species considered by the latter authors was *Minchinia* sp. found in the mud crabs, *Eurypanopeus depressus* and *Rhithropanopeus harrissi*, about 100 miles north of the York River. They also noted its similarity to *M. louisiana*, but reserved judgement on a species designation until further study. No spore dimensions were given.

This paper is concerned with the fine structure of sporulation in the third or possibly fourth species of *Minchinia* thus far studied at the ultrastructural level. Special attention is given to the extraspore wall ornaments, haplosporosomes, and implications of the ultrastructural data in life cycle studies.

Frank O. Perkins is with the Virginia Institute of Marine Science, Gloucester Point, VA 23062. This paper is Contribution No. 687 of the Virginia Institute of Marine Science.

MATERIALS AND METHODS

The fine structure of *Minchinia* sp. sporulating stages was examined in samples of hepatopancreas and musculature from five specimens of *Panopeus herbstii* mud crabs. Two crabs with heavy infections of plasmodia, but without sporulation stages, were also examined. One mm^3 blocks of minced organs were fixed 30 min in 2.5 percent glutaraldehyde buffered at pH 7.2-7.4 with 0.2 M Millonig's phosphate buffer. After three 10 min rinses in the same buffer with 0.15 M NaCl, the blocks were postfixed for 3 h in 1 percent OsO_4 containing 0.1 M Millonig's phosphate buffer (pH 7.4) and 0.2 M NaCl. All solutions were 22-24°C. Dehydration was accomplished in a graded series of ethyl alcohol and embeddings were made in Epon 812[1]. Sections were stained 45 min in a saturated aqueous solution of uranyl acetate followed by 10 min in Reynolds lead citrate. Permanganate fixations were made in 1.2 percent $KMnO_4$ in estuarine water (ca. 20‰ salinity) for 10 min followed by dehydration and embedding as described above.

Whole mounts of spores were prepared for scanning electron microscopy by shaking minced hepatopancreas in estuarine water, centrifuging to separate spores from other cells and cell particulates, fixing in the glutaraldehyde solution described above, and rinsing in distilled water. Rinsed spores were placed on a coverslip fragment, immersed in liquid Freon 22 for 15 sec, then into liquid nitrogen followed by freeze drying on a brass block which had been temperature equilibrated in liquid nitrogen. The spores were then shadowed with gold-palladium and examined at 25 KV.

For light microscopy infected crab organs were placed in Davidson's fixative (Shaw and Battle, 1957) for 2-3

[1]Mention of trade names does not imply endorsement by the National Marine Fisheries Service, NOAA.

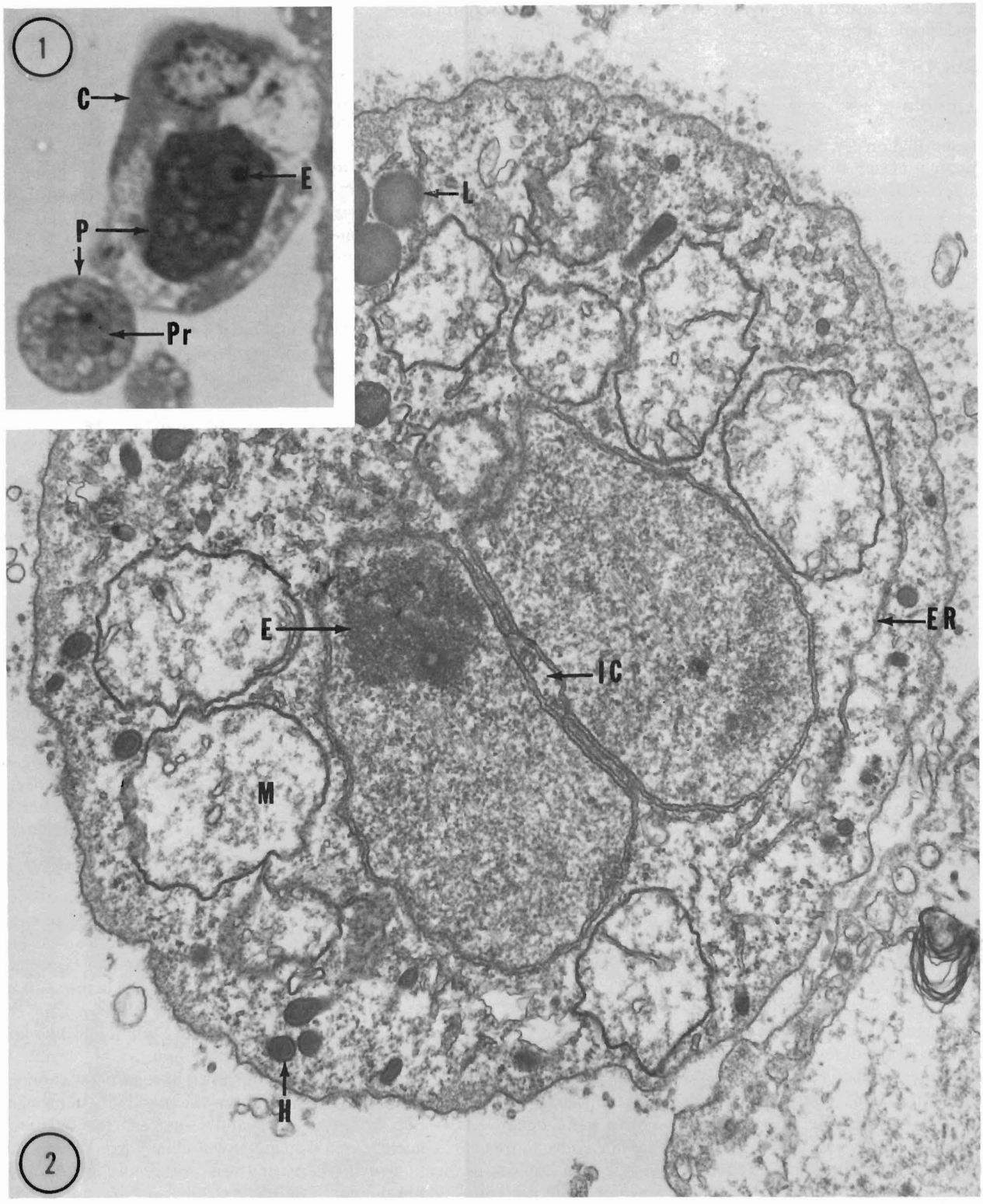

Figure 1[2].—Brightfield micrograph of *Minchinia* sp. plasmodia (P). Crab haemocyte (C); endosome (E); paired nuclei (Pr). 2,200×. Figure 2.—Plasmodium with paired nuclei. Endosome (E); haplosporosome (H); mitochondrion (M); lipoid droplet (L); internuclear chamber (IC); smooth endoplasmic reticulum (ER). 28,000×.

days and embedded in Paraplast (Sherwood Medical Industries, Inc.). Sections were stained in Harris' haematoxylin and counterstained in eosin Y. Measurements of sporont nuclei were made to the nearest 0.2 μm using 3 μm thick sections of the Epon-embedded material stained in aqueous 1 percent toluidine blue adjusted to pH 11 with 1 N NaOH. Plasmodial nuclei were measured to the nearest 0.2 μm using sections of paraffin-embedded material.

[2]Unless otherwise indicated all figures are electron micrographs and all specimens were fixed in glutaraldehyde followed by osmium tetroxide.

Spores were measured from living cells in fresh preparations.

RESULTS

Plasmodia

Presporulation cell types consist predominately of approximately spherical or spheroidal, uni- or binucleate plasmodia without a delimiting wall and measuring from 4.0 to 9.0 μm in longest axis after fixation. The largest plasmodia contained up to 24 nuclei and were as large as 19 μm in longest axis after fixation. Nuclei of all plasmodia were from 1.6 to 8.0 μm diameter (N = 94). Only 14 percent of the nuclei were greater than 3.0 μm diameter (Fig. 10). Those which were about 4.0 μm or larger had nucleoplasm of low staining density in haematoxylin- and eosin-stained sections. Whether they represented nuclei which enlarged during fixation in Davidson's or were reflections of the actual sizes was not determined. They were never observed in glutaraldehyde- and osmium tetroxide-fixed cells; however, that may be due to the smaller numbers of cells seen in the Epon-embedded material. A few of both the 2.2-3.0 μm size nuclei and the large vesicular-type nuclei were observed to be in division.

Generally the nuclei of binucleate plasmodia were found pressed together (Figs. 1-3) with the nuclear envelopes separated by a 30-36 nm wide zone along the opposed surfaces except near the center where the envelopes are infolded forming a cytoplasmic chamber as wide as 1.1 μm between envelopes (Fig. 3). Between opposed portions of the envelope, cisternae of the smooth endoplasmic reticulum were often found. They were generally small vesicles or fragments of flattened cisternae. Although it was not illustrated in previous papers (Perkins, 1968; 1969; 1971), I observed the same structural characteristics for paired nuclei of *M. nelsoni*, *M. costalis*, and *U. crescens*. A single, generally spherical, and Feulgen-negative endosome was found against the nuclear envelope of *Minchinia* sp. Secondary clumps of basophilic, Feulgen-positive material were scattered in the nucleoplasm.

The cytoplasm included lipid-like droplets, mitochondria, and a sparse array of smooth endoplasmic reticulum (Fig. 2). An anastomosing reticulum of cisternae was also found in many cells (Fig. 3). Whether it represented a modified Golgi body was not determined. Haplosporosomes (Figs. 2-5) (Perkins, 1971) were scattered throughout the cytoplasm as already observed in *M. nelsoni*, *M. costalis*, and *U. crescens*. The inclusions of *Minchinia* sp. did not appear to arise from generative regions as was presumed to occur in *M. nelsoni* (Perkins, 1968) nor were the haplosporosomes similar in shape to those in other haplosporidans. Those of *Minchinia* sp. were club-shaped (Fig. 4) with the head of the club ranging from 129 to 186 nm diameter ($\bar{X}$ = 155; N = 11; $S_{\bar{X}}$ = 6); the "handle" diameter, from 84 to 117 nm ($\bar{X}$ = 95; N = 7; $S_{\bar{X}}$ = 5); and the overall length, from 300 to 586 nm ($\bar{X}$ = 456; N = 7; $S_{\bar{X}}$ = 37). It is not known, however, whether some of the profiles which were assumed to be cross-sectional views could have represented medial sections of spheres or spheroids. The haplosporosomes had a three-part substructure consisting of two electron-dense zones separated by a thin electron-light zone as already described in the other species and were delimited by a unit membrane. The internal electron-light zone proved to have a tripartite substructure when fixed in potassium permanganate (Fig. 5). Each plasmodium had fibrogranular material adhering to the surface (Fig. 6), but no wall as appears during sporulation (Fig. 8).

Nuclear division occurs without nuclear envelope breakdown and with the involvement of a persistent mitotic apparatus. The latter was found in 76 percent of 75 nuclear profiles counted; therefore, it is assumed that interphase nuclei contain the apparatus. A positive sighting was considered to be a group of five or more microtubules. Only nuclei that did not show evidence of lengthening and pinching in half were counted. The mitotic apparatus consists of two spindle pole bodies embedded in the nucleoplasm free of the nuclear envelope or in some cases touching on the envelope, but not embedded in the envelope or in the cytoplasm. A bundle of microtubules connects the two bodies (Fig. 7). Upon division the nucleus changes from a sphere to a spheroid, lengthens further into a dumbbell-shaped unit, then pinches in half. The microtubular bundle lengthens as division proceeds.

Sporont

Upon initiation of sporulation, the plasmodia increase in mass and number of nuclei. Whether this is a result of plasmogamy was not determined. A wall about 23 nm thick is formed around each cell and persists until spore maturation and release (Fig. 8). In spite of its size, the wall can be seen in the light microscope when the cytoplasm separates from it, because adhering fibrogranular material increases the apparent thickness and both "layers" stain deeply in toluidine blue (Figs. 16 and 17). Upon addition of the wall, the plasmodia are herein considered to have developed into sporonts until sporoplasm delimitation occurs at which time they are termed sporocysts. Sporonts were 22-71 μm (N = 20) in longest axis and had the same general shape as plasmodia. The cytoplasm resembled that of plasmodia except that haplosporosomes disappeared from the cytoplasm and few lipoid bodies were observed.

Sporont nuclear division was identical to that in plasmodia and the division apparatus (microtubules and spindle pole bodies) appeared to persist through interphase as in plasmodia. Although nuclear division figures were observed, it was not determined how many division cycles occur after the cells become sporonts. It is suspected, however, that at some point karyogamy occurs followed by meiosis. Nuclear sizes varied from 2.3 to 5.9 μm diameter (N = 275) with most individual sporonts containing nuclei of one limited size range ($\pm$ ca. 0.5 μm) not mixed sizes. However, a few sporonts had large nuclei and small paired nuclei in the same cell. In Figure 9 there is one pair of small nuclei (2.5 and 2.9 μm) and five larger nuclei (4.1-4.6 μm; $\bar{X}$ = 4.4 μm). The section shown in Figure 9 was one of a series, thus the possibility of measuring significantly less than the full nuclear diameter was eliminated. When nuclear pairing was observed it nearly always involved small (< 3.0 μm) nuclei. "Pairing" is considered to exist when the opposed surfaces of paired nuclei are flattened as in Figures 1 (lower pair of nuclei) and 2.

Since there appeared to be a possibility that karyogamy occurs in the sporonts, nuclear diameters were examined in an effort to see if a bi- or trimodal size

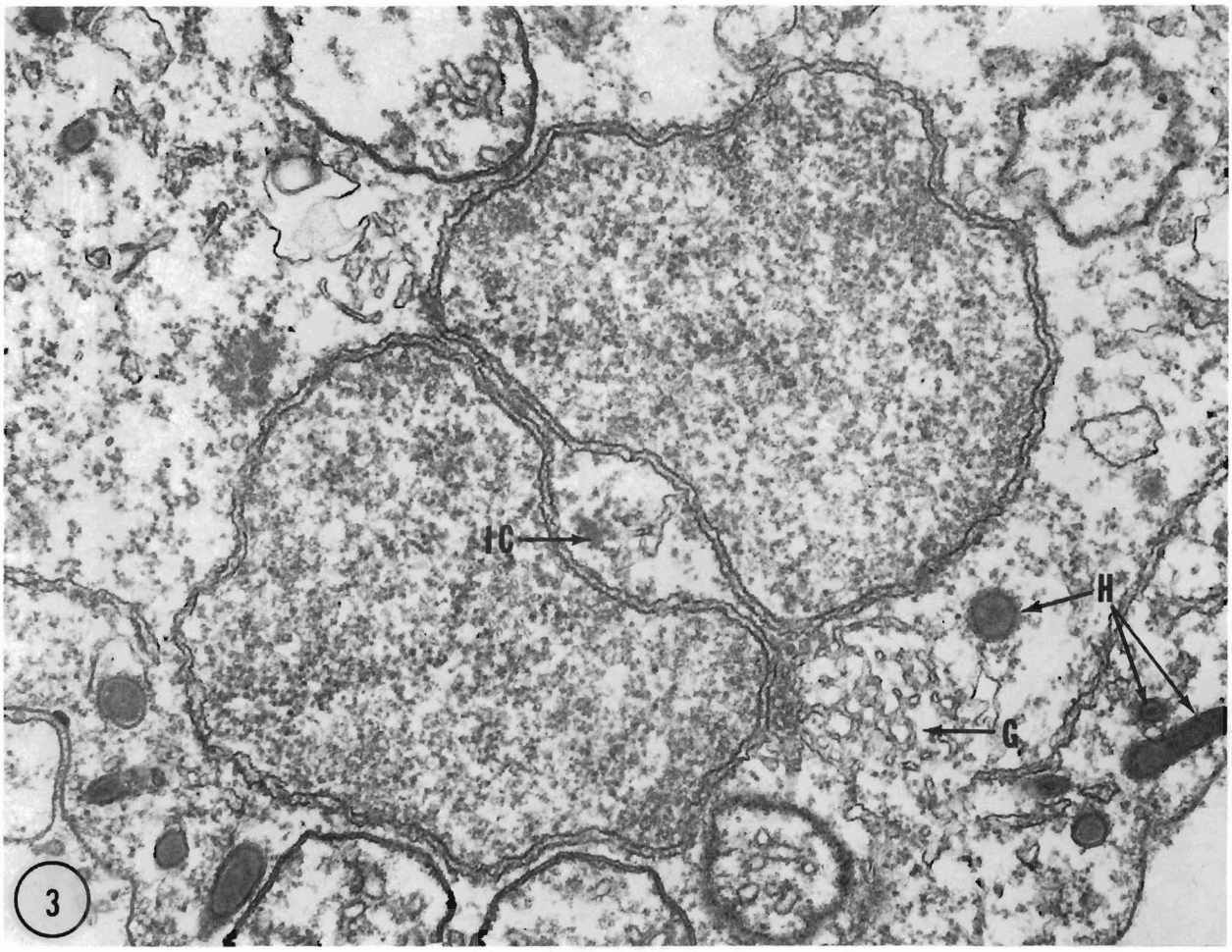

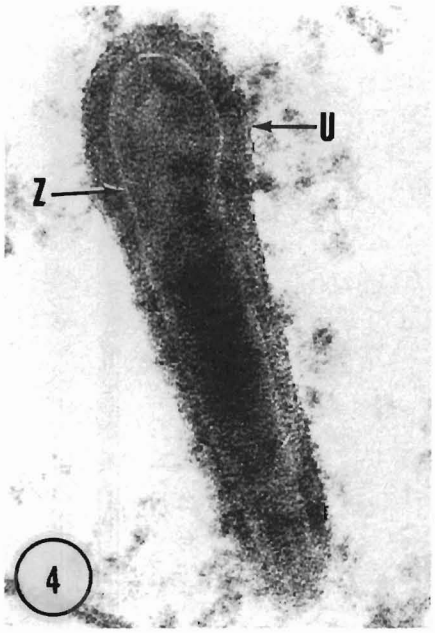

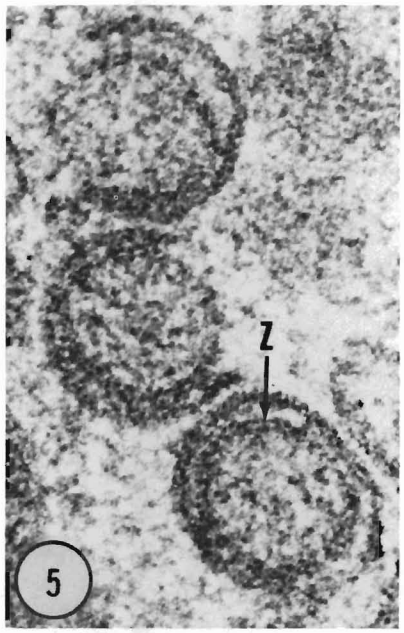

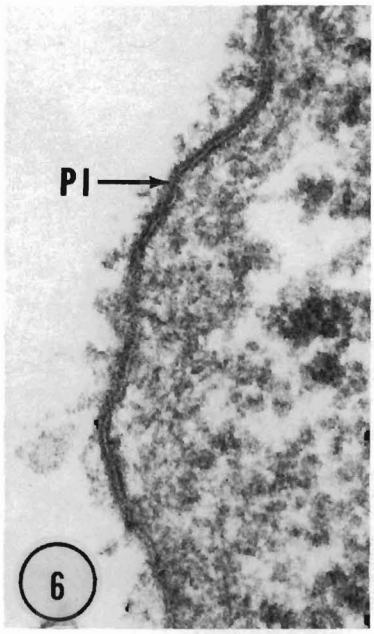

Figure 3.—Paired nuclei in plasmodium. Note internuclear chamber (IC); haplosporosomes (H); Golgi-like body (G). 35,000×. Figure 4.—Haplosporosome in plasmodium. Note characteristic substructure consisting of two electron-dense regions separated by an electron-light zone (Z). The inclusions are delimited by an unit membrane (U). 168,000×. Figure 5.—Haplosporosomes fixed in potassium permanganate. Note that electron-light zone (Z), seen in Figure 4, appears to have a tripartite substructure like a unit membrane. 180,000×. Figure 6.—Plasmalemma (PI) of plasmodium. 127,000×.

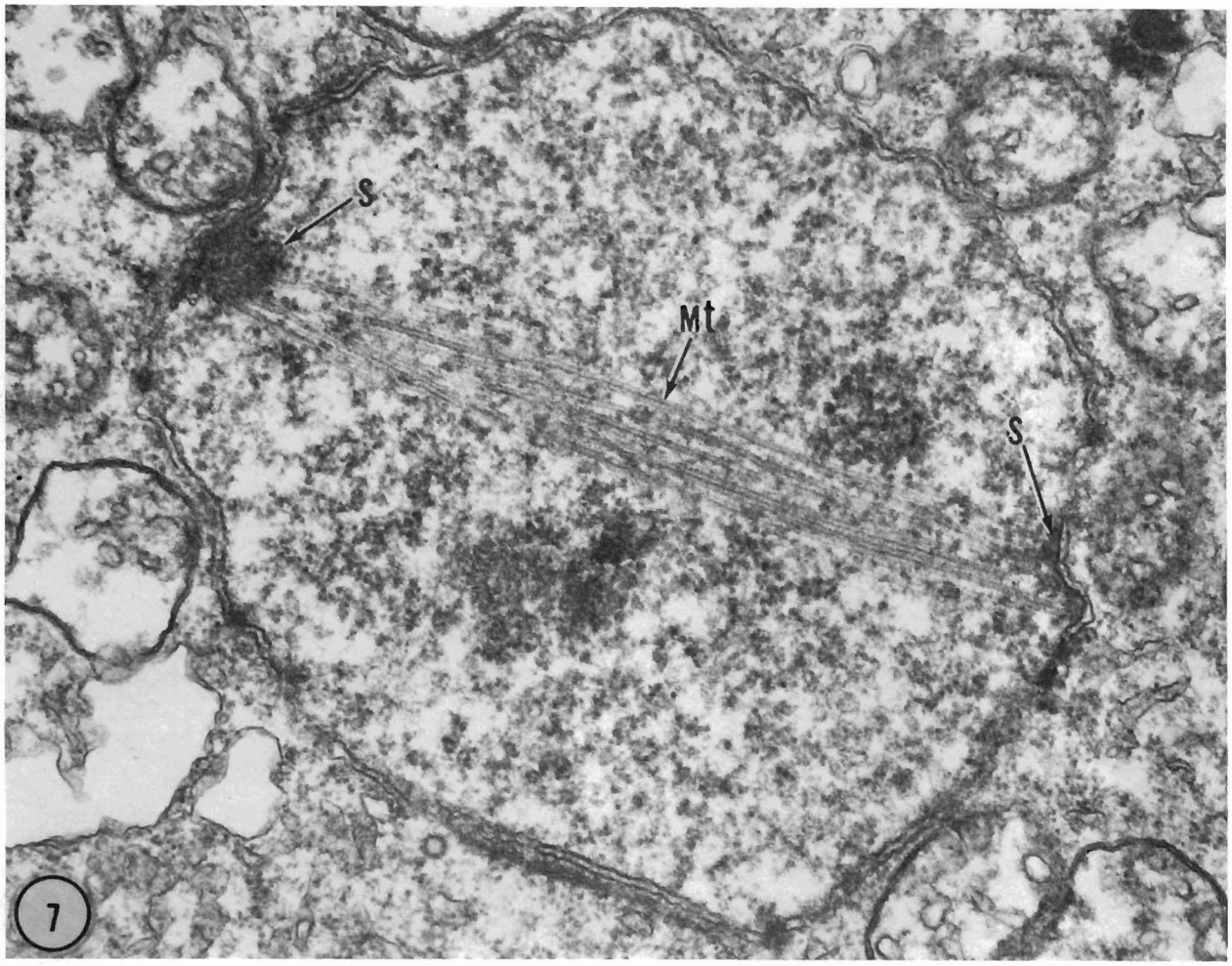

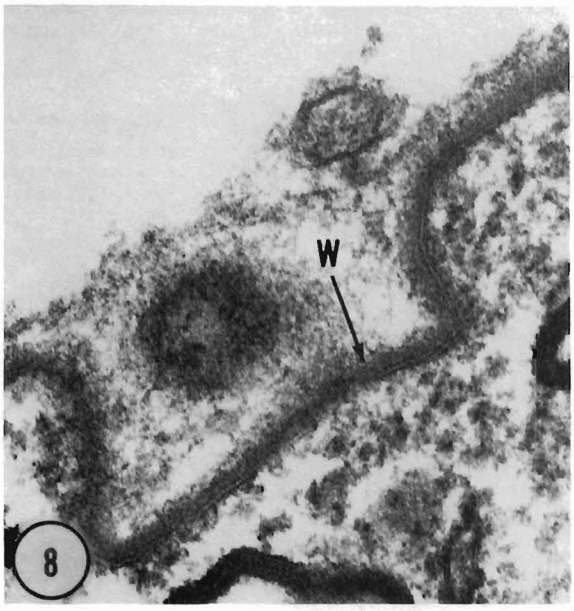

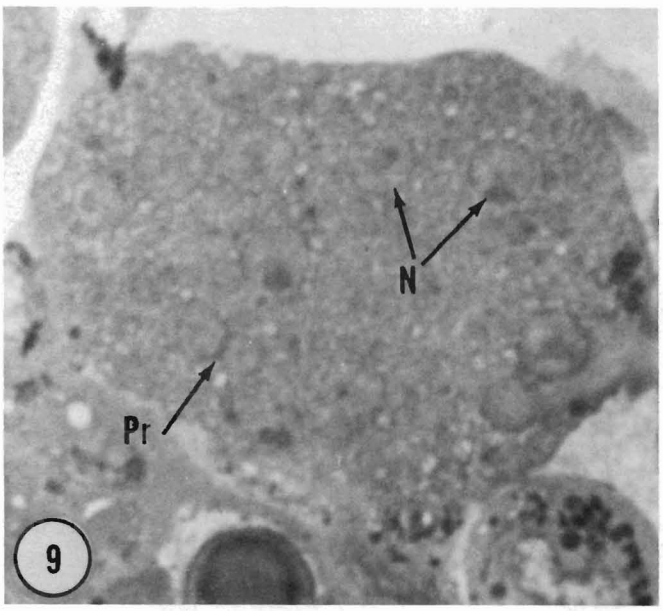

Figure 7.—Mitotic apparatus of plasmodial nucleus consisting of two spindle pole bodies (S) connected by a bundle of microtubules (Mt). Spindle pole body on the right is tangentially sectioned. 36,000×. Figure 8.—Plasmalemma and wall (W) of uncleaved sporont. 110,000×. Figure 9.—Brightfield micrograph of sporont in which a pair of small nuclei (Pr) and several large nuclei (N) are visible. It is believed that at this stage pairing of small (2.5-3.0 *um*) nuclei occurs followed by karyogamy to yield larger (4-4.5 *um*) nuclei. 2,100×.

distribution could be observed; however, when 275 nuclear diameters from 50 sporonts were represented in histograms, no clear evidence of polymodal distributions was observed, only a skewed distribution with one obvious mode. One such histogram with the data plotted at 0.2 μm intervals is shown in Figure 10. Two modes may be present, but they are not definitive.

Structures presumed to be synaptonemal complexes (SC's) and polycomplexes (PC's) were observed in sporont nuclei (Figs. 11-13). Thus meiosis is suspected to occur. The presumptive medial complex or ribbon appeared as a granular band in some sections (Fig. 11) (group B type of SC; Wettstein and Sotelo, 1971), or as a multilayered structure (Fig. 12) (group C type of SC). Differences in structure may have been due to variations in resolution and fixation quality. The medial space between lateral elements was about 67 nm wide. SC-like structures were not observed in nuclei of plasmodia, sporocysts, or spores, nor were they seen in paired or obvious anaphase and telophase nuclei of sporonts (Fig. 14).

Polycomplex-like structures consisted of from 3 to 9 electron-dense bands in parallel arrays separated by electron-light zones 15-51 nm wide (N = 9; $\bar{X}$ = 24; $S_{\bar{X}}$ = 4). The spaces varied greatly in size from complex-to-complex but within a given complex the spacing varied little (Fig. 13). The dense bands were 44-50 nm thick (N = 9; $\bar{X}$ = 46; $S_{\bar{X}}$ = 0.8). Complexes were found only in sporont nuclei and never in nuclei with the presumptive SC's. Due to the problems associated with identifying nuclear size from thin sections, it is not known whether the suspected SC's and PC's were found only in large (4 to 6 μm diameter) nuclei; however, it is known that at least some of the nuclei were in that size range (Fig. 15).

After sporont cleavage is initiated no further nuclear divisions occurred. Cytokinesis occurred in two ways, both of which were commonly observed. The more ordered pattern of cleavage resulted from peripheral and internal partitioning to yield a syncytium (Fig. 16). Further cleavage resulted in approximately spherical, uninucleate sporoblasts. Another type of cleavage which appeared to be aberrant, but which was observed as frequently, consisted of cleavage and delimitation of approximately spherical, uni- or, sometimes, binucleate sporoblasts and sporoplasms from the sporont at large. Delimitation occurred at the sporont periphery as well as internally thus forming free cells within the sporont wall, cells in invaginations of the sporont surface, and cells in vacuoles within the sporont (Figs. 17-20). Since synchronous delimitation does not occur, numerous stages of development are observed within a given sporont—from nearly mature spores to cleaving multinucleated fragments of sporont cytoplasm (Fig. 20). Obviously aberrant as well as a few normal-appearing spores (Figs. 17 and 20) were formed in these sporonts; therefore, the first cleavage sequence described above appears to result in formation of most of the spores since the sporocysts with large numbers of mature spores rarely contained any aberrant ones.

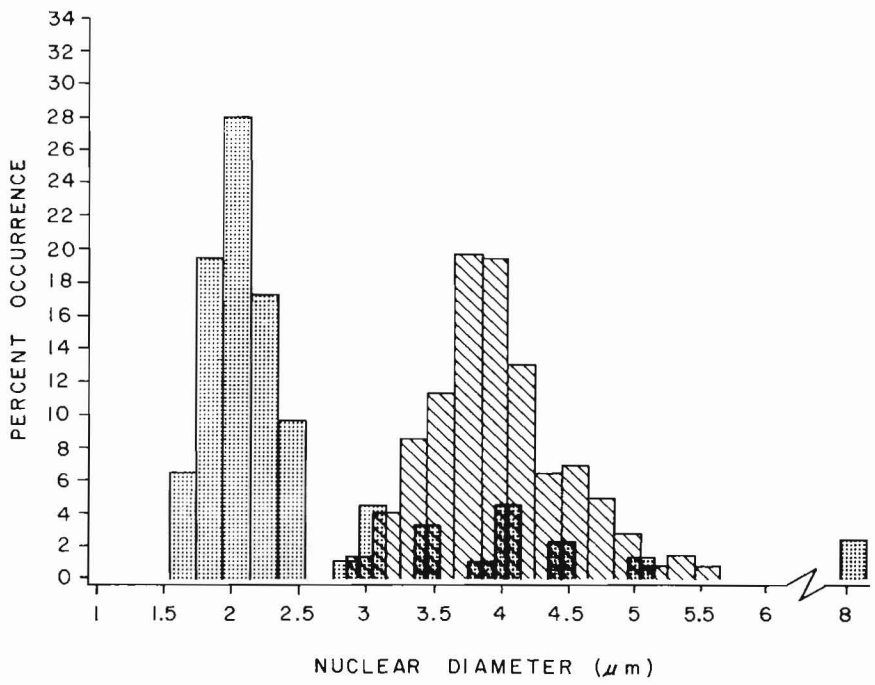

Figure 10.—Histogram showing distributions of nuclear diameters of plasmodia (dotted bars) and sporonts (hatched bars).

Sporocyst

Upon delimitation of the sporoplasm within sporoblasts the sporont is herein considered to be a sporocyst. I was not able to determine how separation of sporoplasm from the rest of the sporoblast cytoplasm occurred. Presumably it was formed by invagination of the sporoblast plasmalemma and/or fusion of cytoplasmic vesicles. Partial separation of sporoblasts into sporoplasm primordia and "envelope" primordia was not observed nor were degenerate nuclei seen; therefore, the scheme proposed by Ormières et al., (1973) is probably not descriptive of sporoplasm delimitation in *Minchinia* sp. (see "Discussion"). Cup-shaped units of anucleate cytoplasm, each partially surrounding a sporoplasm primordium, were observed in *Minchinia* sp., but their subsequent development was not determined.

As noted in my previous papers, spore wall formation occurs in the extrasporoplasm cytoplasm. A thin layer of electron-dense material was deposited on the outer surface of the extrasporoplasm cytoplasmic membrane which parallels the sporoplasm plasmalemma (Fig. 21). Subsequent additions of material yielded a laminated thick wall, then a final layer of electron-dense material was added to yield a corrugated surface (Fig. 22). The outermost layer appeared to form by fusion of long, 44-67 nm diameter ($\bar{X}$ = 55; N = 20; $S_{\bar{X}}$ = 1.4) strands of electron-dense material to the laminated spore wall or possibly from material similar to the strands, deposited in some other form (Fig. 23). The strands were apparently formed in vacuoles in

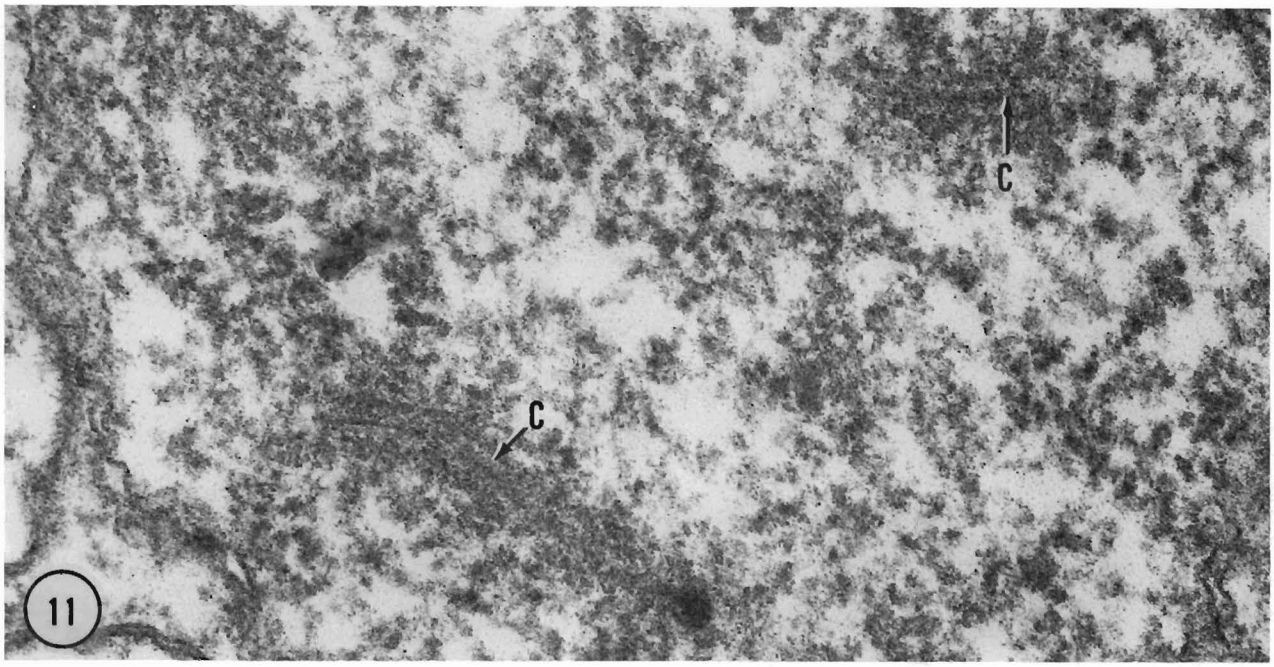

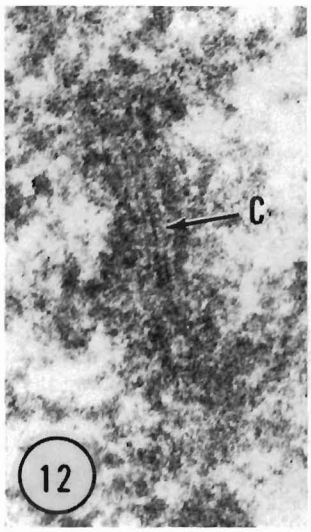

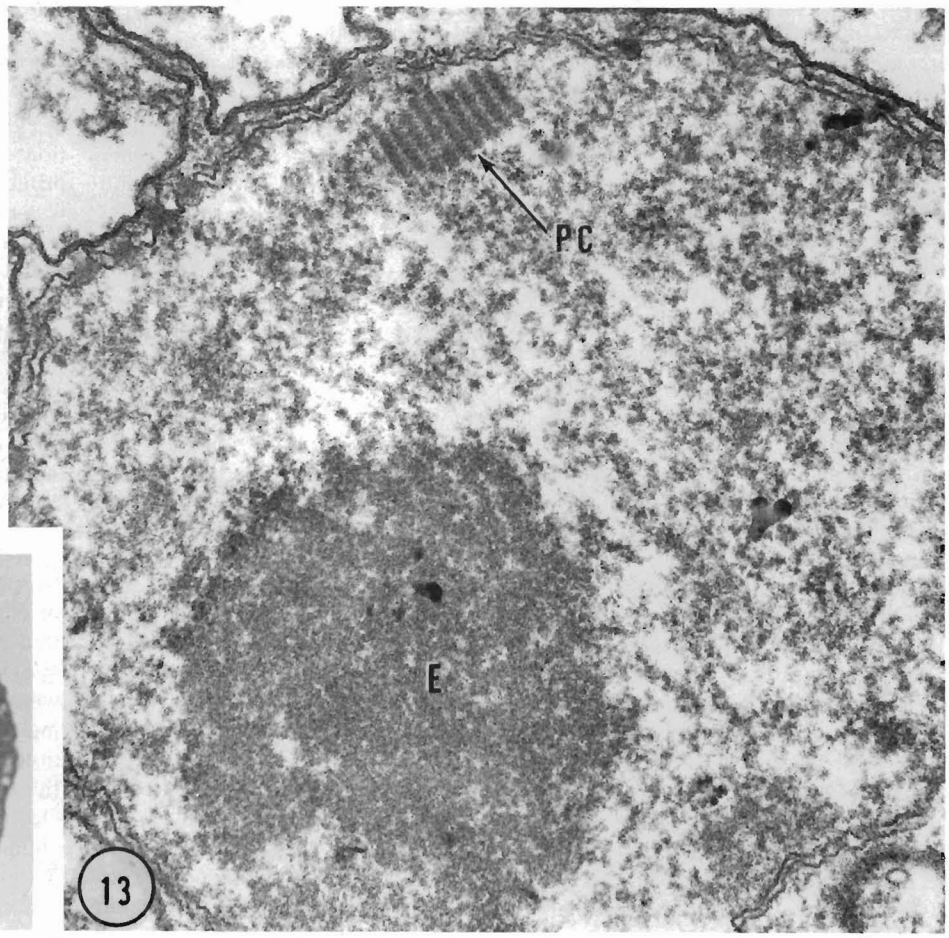

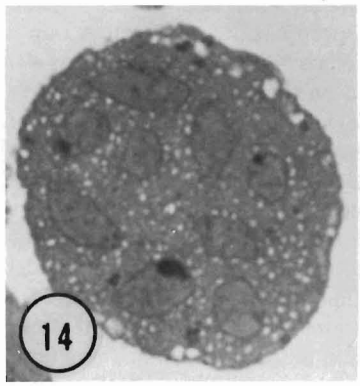

Figures 11 and 12.—Synaptonemal complex-like structures in sporont nuclei. Medial complexes (C) in Figure 11 are granular bands and the one in Figure 12 is multilayered. Figure 11: 49,000×; Figure 12: 70,000×. Figure 13.—Polycomplex-like structure (PC) in sporont nucleus. Endosome (E). 35,000×. Figure 14.—Brightfield micrograph of sporont showing nearly synchronous division of large (4-5.5 *um*) diameter nuclei. 1,200×.

the extrasporoplasm cytoplasm. Vacuolar contents first appeared as a fibrogranular mass which then differentiated into parallel arrays of ca. 22 nm diameter tubules (Fig. 24). It is suspected that the latter then developed into the strands or wrappings, but intermediate stages were not visualized. Strands were either fused to the spore wall or wrapped loosely around the wall. Surface views of the mature wall (Fig. 25) showed strands as units of considerable length (greater than 10 μm) when unwound. Distally the strands appear to be about 50 percent of the proximal diameter, but this was not detected in the sectioned material.

Anteriorly the spore wall was flared forming a flange which was continuous at one side with a lid, as previously described in the other species of *Minchinia*. The lid rested on the flange and covered a pore in the spore case (Fig. 26). Thus the lid was hinged along one side (Fig. 26) and not continuous with the flange along the opposed side (Fig. 27). The plasmalemma delimiting the extrasporoplasm cytoplasm was invaginated at the non-hinge side (Fig. 27) and was continuous with the membrane opposed to the whole spore wall. The plasmalemma of the sporoplasm was not continuous with the membrane which was opposed to the wall. Interconnecting strands connected the flange and lid at the non-hinge side until later development led to partial fusion of lid and flange (Fig. 22).

By the time of sporoplasm delimitation, the Golgi body had appeared at the nascent anterior end of the spore. As previously described in other species (Perkins, 1968, 1969, 1971; Rosenfield et al., 1969), it consisted of convoluted, anastomosing cisternae which initially contained little or no dense material. As spore maturation proceeded, the cisternae filled with electron dense material in some regions. The material was released into the cytoplasm as membrane-bound inclusions with parallel bands of electron-dense material (Fig. 28). Haplosporosomes reappeared in the cytoplasm of developing spores from the membrane-bound inclusions, apparently budding from the periphery of the inclusion, thereby deriving a delimiting membrane from the inclusion membrane (Figs. 28 and 29). Haplosporosomes were pyriform, not club-shaped as in the plasmodia, and were

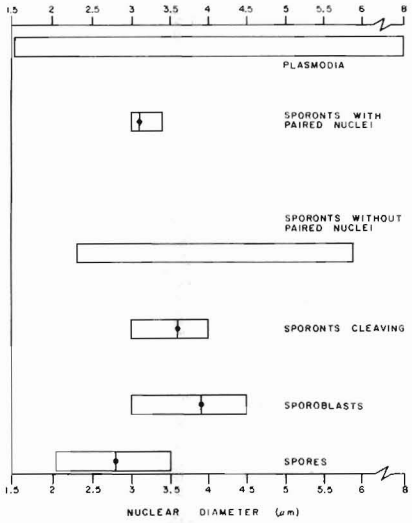

Figure 15.—Comparison of ranges and means of nuclear diameters of various cell types in sporulation sequence. No mean is given for uncleaved sporonts, because it is suggested that karyogamy followed by meiosis occurs in the sporonts; thus the nuclei of several cell stages have been unavoidably measured as one stage. The mean for plasmodia was omitted, because of uncertainties concerning the significance of the large vesicular nuclei (see "Discussion" section).

104-151 nm diameter ($\bar{X}$ = 124; N = 20; $S_{\bar{X}}$ = 2.9) through the globose portion. Both formative inclusions and free haplosporosomes were concentrated in the equatorial region of the spore. A few lipoid bodies, mitochondria, and cisternae of smooth endoplasmic reticulum were scattered throughout the cytoplasm.

There was only one nucleus per sporoblast, developing spore, and mature spore except in rare, presumably aberrant, cases where two were observed in the first two stages, but not in mature spores. The two nuclei were often in a paired configuration as seen in developing sporonts; therefore, the possibility that pairing does not represent prekaryogamy orientation must be considered. However, binucleate sporoblasts and spores were seen only in sporonts cleaved in the presumably aberrant manner (see previous "Sporont" section). Nuclear size decreased back to approximately that of the most commonly observed, non-vesicular plasmodial nuclei (Fig. 15). The mitotic apparatus, persistent in plasmodial nuclei up to sporoblast delimitation, was not in spore nuclei or in sporoblasts where sporoplasm delimitation had occurred.

As with the other species of *Minchinia* and *Urosporidium* studied, spore maturity yielded spores with high electron density which were relatively impervious to fixatives and embedding media; therefore, fully mature sporoplasms were not viewed in detail in sectioned material. Freeze-etch replicas indicated that little further structural modification in the sporoplasm occurred, only dehydration as evidenced by degree of sublimation during freeze-etching.

In interference optics the nucleus, Golgi body, and concentration of inclusions were visible in living spores (Fig. 30). The three were also visible in sectioned, stained spores (Fig. 31).

After formation of uninucleate sporoblasts, the sporoplasm is delimited followed by spore wall formation then loss of the extrasporoplasm cytoplasm except for the wall wrappings (Fig. 25). The fate of the spores is unknown.

DISCUSSION

As Andrews (1966) has noted in his extensive epizootiological studies of *Minchinia nelsoni*, the life cycle of this oyster pathogen is poorly known. An important factor in this dearth of information is inability thus far to identify the reservoir of infective elements. The present study was, in part, initiated to determine whether the fine structure of *Minchinia* species in *Panopeus herbstii* resembled *M. nelsoni*. The mud crab is commonly found associated with oysters and, therefore, is a logical organism to consider as an alternate host.

Evidence from the comparative fine structure of the two parasites indicates that they are distinct species. They differ in the following respects: 1) *M. nelsoni* plasmodia have large formative regions for haplosporosomes (Perkins, 1968), none are seen in *Minchina* sp.; 2) haplosporosomes are club-shaped in *Minchinia* sp., spherical in the oyster pathogen; 3) large numbers of haplosporosomes are found in spores of the mud crab parasite, but none were readily identified in spores of *M. nelsoni* although electron-dense bodies were present which showed a faint indication of the usual bipartite substructure typical of haplosporosomes; and 4) the strands or wrappings around the spores of *M. nelsoni* were tubular (43-63 nm; $\bar{X}$ = 50 nm diameter) with a cartwheel-like internal substructure, whereas those of *Minchinia* sp. were electron-dense strands with no discernible substructure although the diameters were similar. At

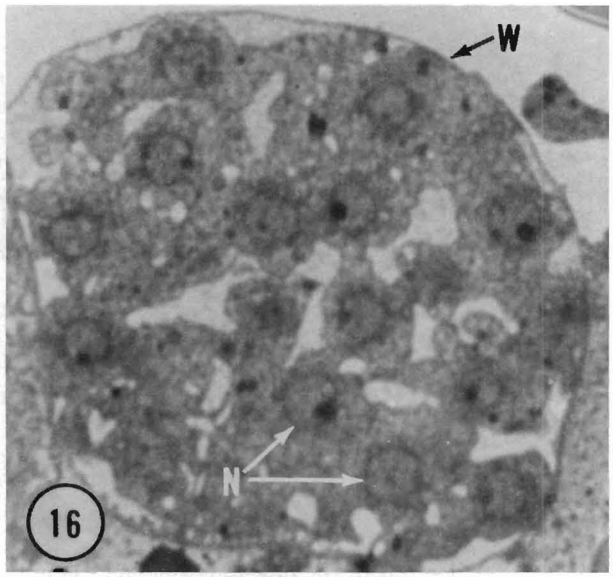

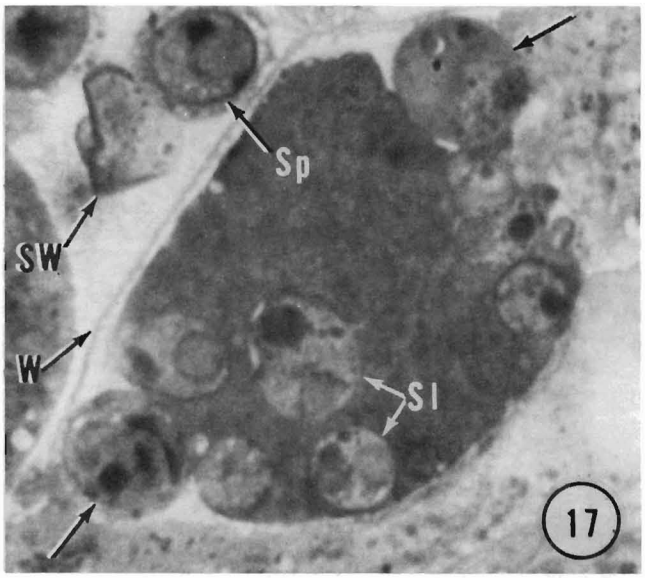

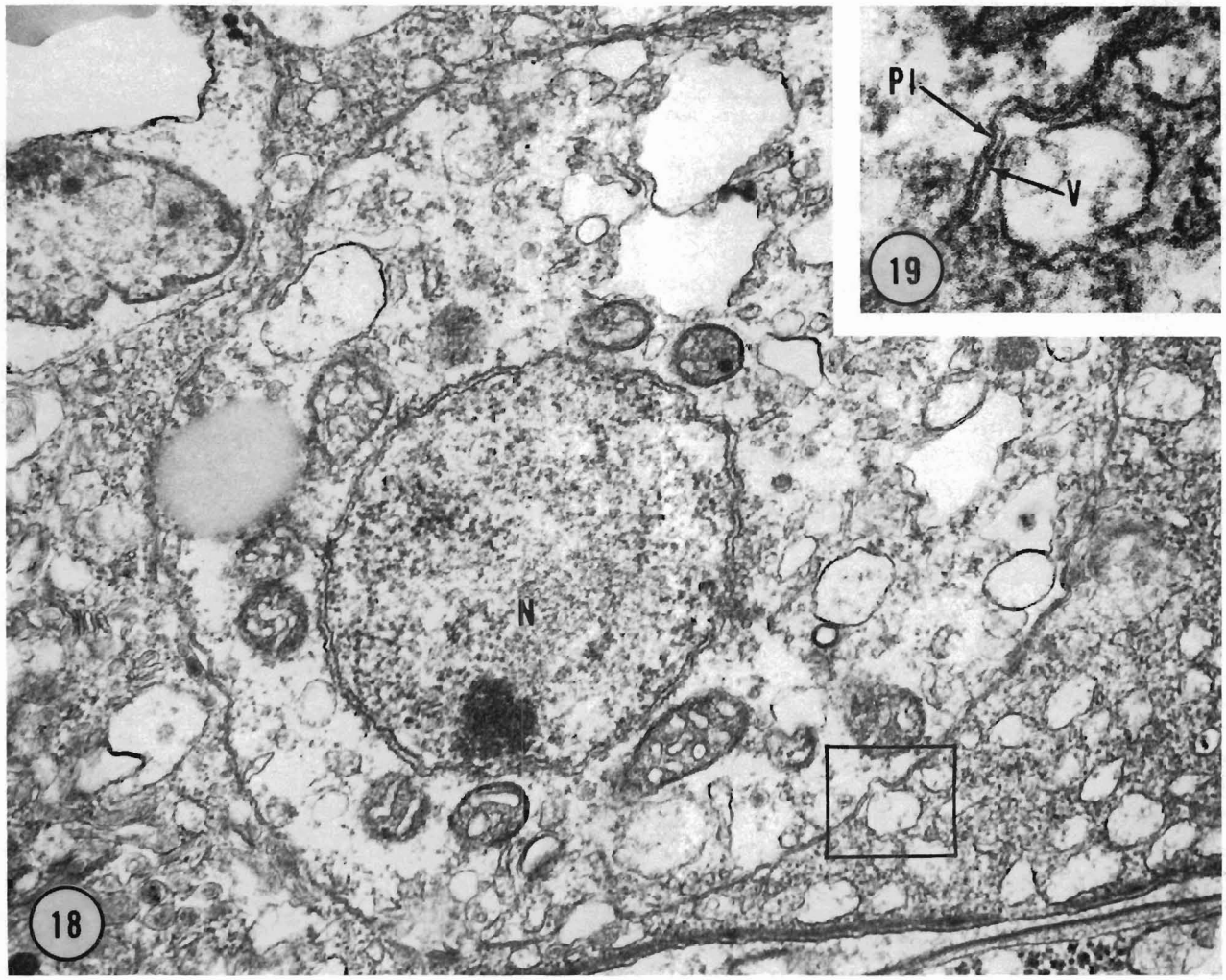

Figure 16.—Multinucleate syncytium resulting from partial internal and peripheral cleavage of sporont. Nuclei (N); sporont wall (W). 1,700×. Figure 17.—Sporont showing aberrant (?) cleavage which yields free uninucleate cells (arrows) and fully delimited sporoplasms (SI). Sporont wall (W); developing spore (Sp); aberrant spore wall (SW). 1,600×. Figs. 18 and 19.—Sporoplasm delimited within sporont which showed aberrant (?) cleavage patterns. Subdivision into sporoblasts had not occurred. Figure 19 is higher magnification of area within square showing sporoplasm plasmalemma (PI) and membrane (V) of vacuole in which sporoplasm is situated. Sporoplasm nucleus (N). Figure 18: 29,000×; Figure 19: 90,000×.

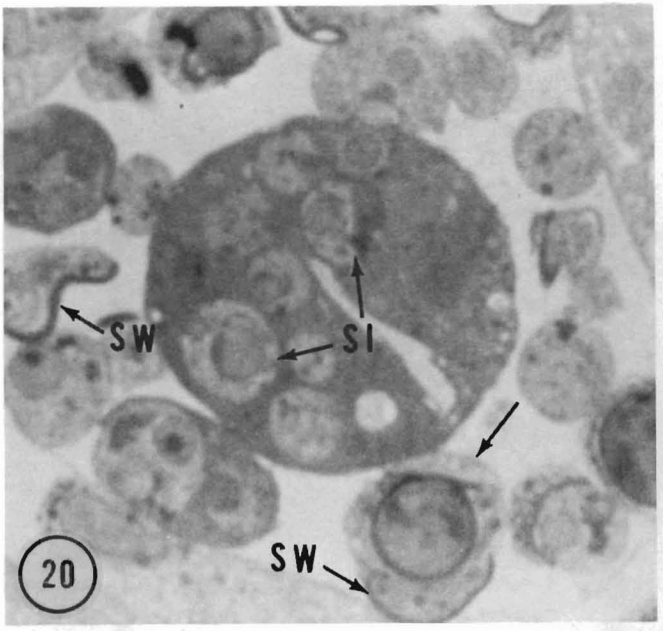

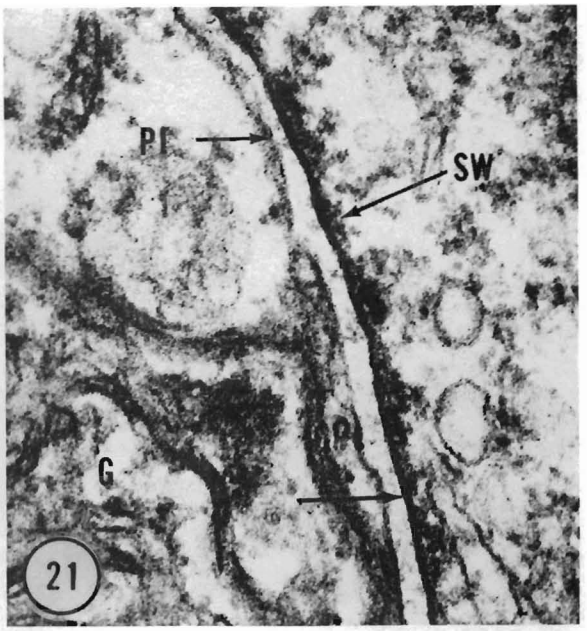

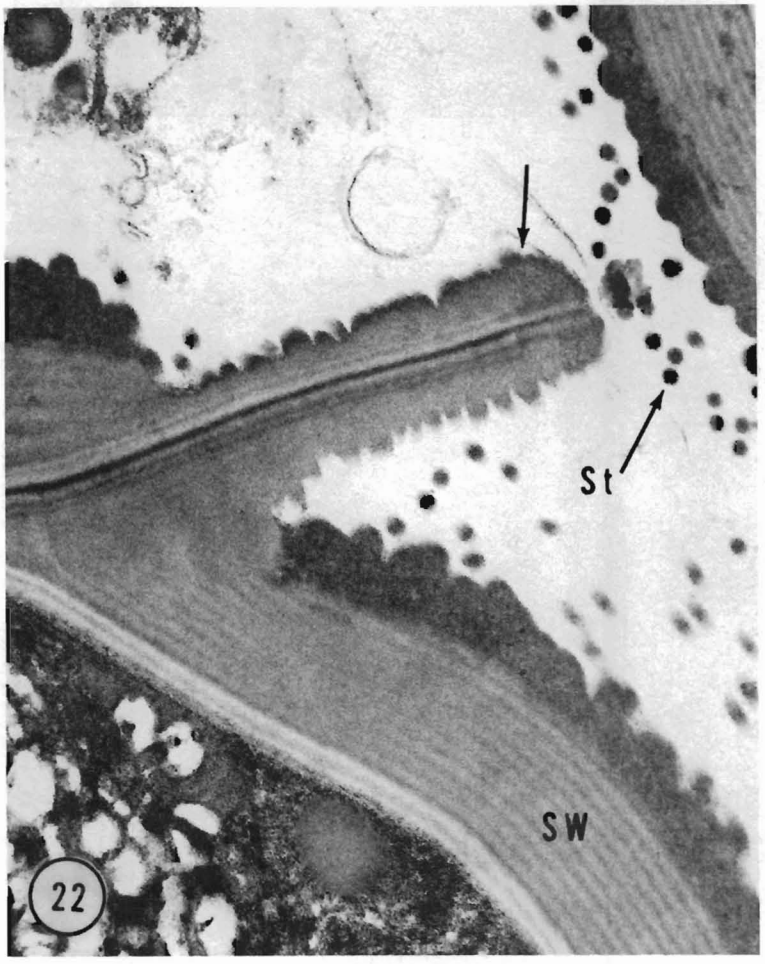

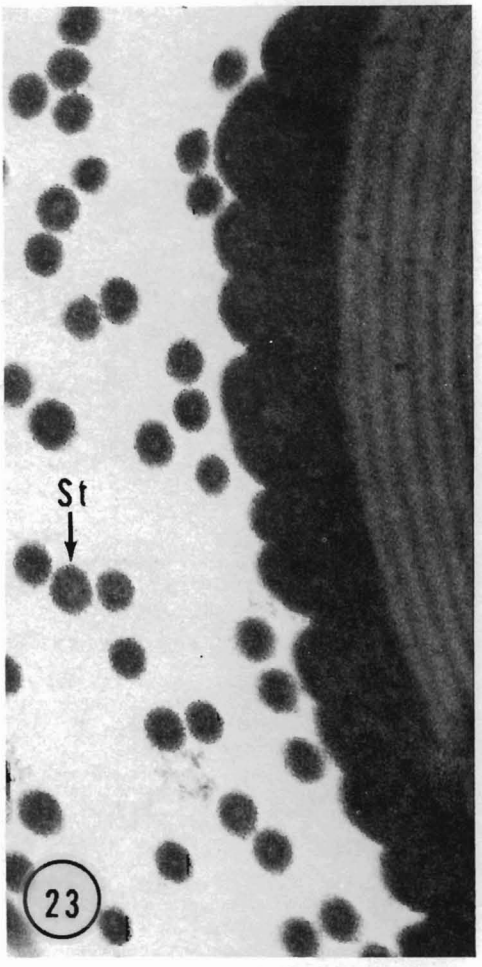

Figure 20.—Brightfield micrograph of cleaving aberrant sporont. Sporoplasms (Sl) have been cleaved from largest mass of cytoplasm. Nearly mature spore (arrow); aberrant spore wall formation (SW). 1,800×. Figure 21.—Initiation of spore wall (SW) formation. Plasmalemma of sporoplasm (Pl); membrane of extrasporoplasm cytoplasm (arrow); Golgi body (G). 77,000×. Figure 22.—Mature spore wall (SW) showing unhinged portion of lid-flange complex (arrow). Strands or wrappings around spore wall (St). 47,000×. Figure 23.—High magnification of spore wall showing corrugated surface and cross sections of strands (St). 106,000×.

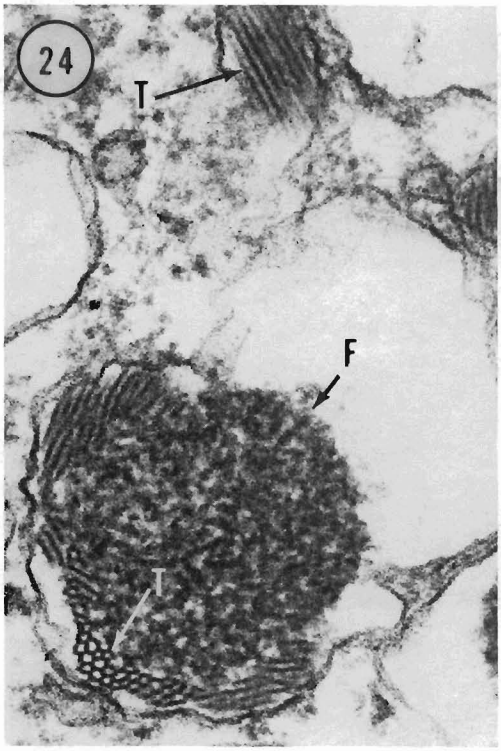

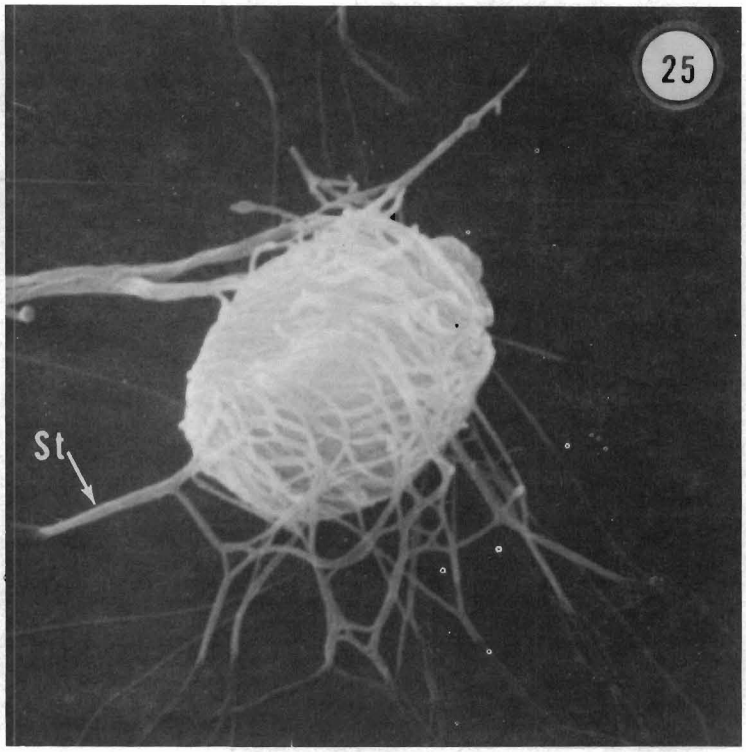

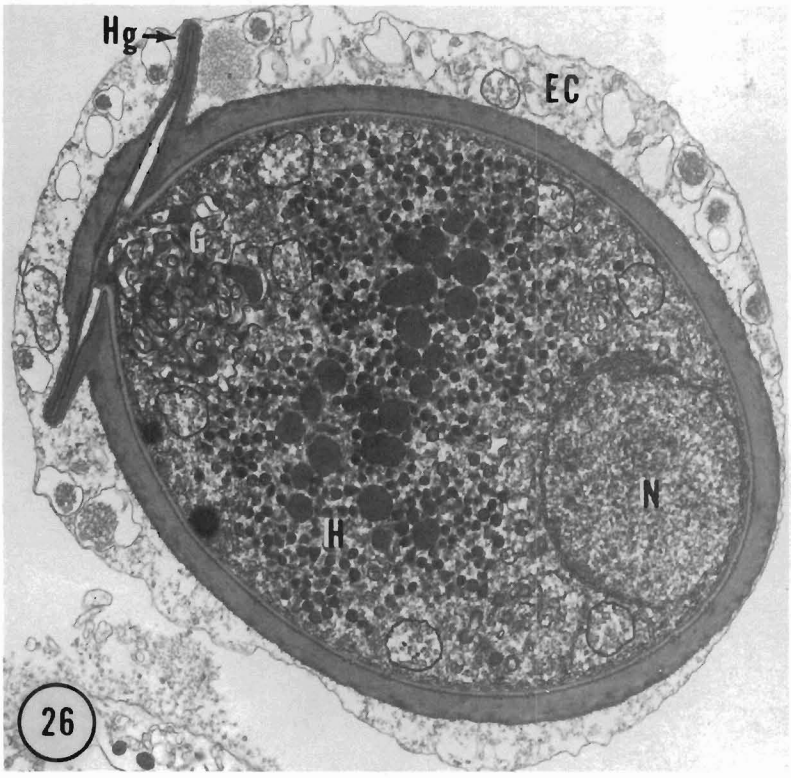

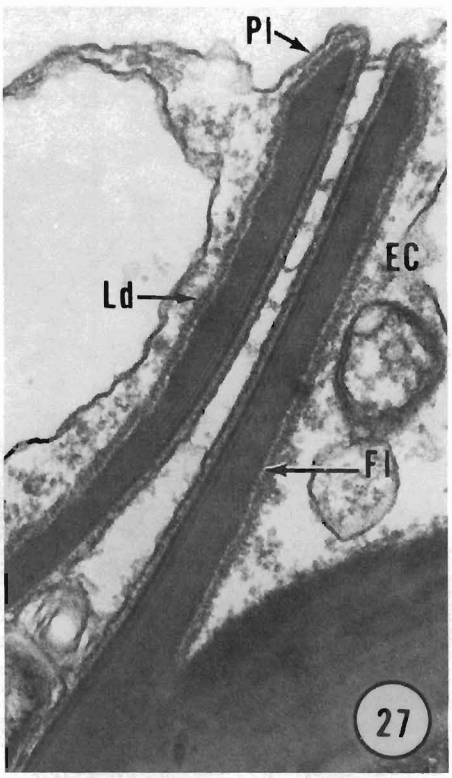

Figure 24.—Fibrogranular material (F) in vacuoles of extrasporoplasm cytoplasm. It is suggested that the material is used in synthesis of the tubules (T) which, in turn, are used in formation of the strands seen in Figures 22 and 23. 70,000×. Figure 25.—Scanning electron micrograph of spore. Note strands (St) or wrappings around spore wall. 5,800×. Figure 26.—Immature spore sectioned through hinge (Hg) region of lid-flange complex. Nucleus (N); haplosporosomes (H); Golgi body (G); extrasporoplasm cytoplasm (EC). 13,000×. Figure 27.—Non-hinge region of lid-flange complex. Note that plasmalemma (Pl) of extrasporoplasm cytoplasm (EC) invaginates and lies at the interface between lid (Ld) and flange (Fl). 57,000×.

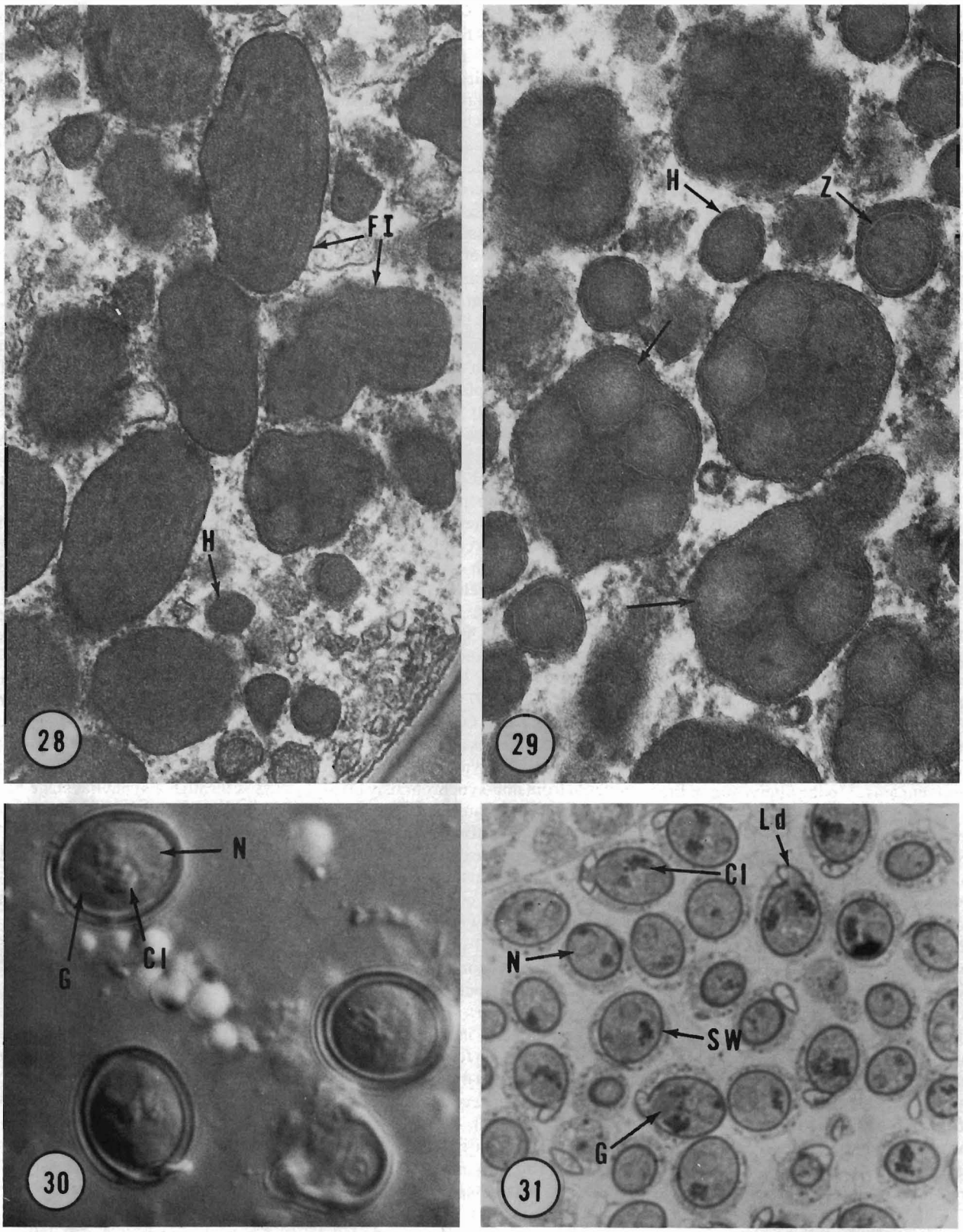

Figure 28.—Formative inclusions (FI) of immature spore in which haplosporosomes (H) are assembled. Inclusions are formed in Golgi body. 66,000×. Figure 29.—Higher magnification of formative inclusions showing haplosporosomes (arrows) being formed. Free, fully-formed haplosporosome (H); electron-light zone (Z) (see Figures 4 and 5). 104,000×. Figure 30.—Nomarski interference micrograph of living spores. Golgi body (G); nucleus (N); cluster of haplosporosomes and formative inclusions (CI). 1,000×. Figure 31.—Brightfield micrograph of sporocyst showing developing spores. Spore wall (SW); nucleus (N); cluster of haplosporosomes and formative inclusions (CI); Golgi body (G); lid (Ld). 1,300×.

the cytological level, the organisms differ in spore size. *M. nelsoni* spores are 6.8-11.4 μm long ($\bar{X}$ = 8.1) and 4.6-6.8 μm wide ($\bar{X}$ = 5.5) (Couch, 1967), whereas *Minchinia* sp. spores are 9.0-10.0 μm long ($\bar{X}$ = 9.6; N = 30) and 7.5-8.5 μm wide ($\bar{X}$ = 8.1; N = 30).

As opposed to the differences there were numerous similarities between the two species in nuclear, mitochondrial, spore Golgi body, and wall structure as well as in mitosis. Species distinctions are admittedly subjective, and it could be argued that the above differences are only apparent due to growth in different hosts. As with most species distinctions, subjectivity of necessity plays a dominant role, as in the present consideration, until adequate information is available. I have used spores from *Minchinia* sp. in attempts to infect oysters, but no infections occurred. However, since neither *Minchinia* spp. nor *Haplosporidium* spp. infections have been experimentally transmitted, this failure can not be considered as significant.

Ormières et al. (1973) proposed an interesting scheme to describe sporoplasm delimitation and spore wall formation in *Urosporidium jiroveci*. They suggested that there are possibly pairs of nuclei in the syncytium of cleaving sporonts in which one nucleus degenerates and the other nucleus becomes the spore nucleus. Upon subdivision of the syncytium into sporoblasts, they suggested that partial division of the sporoblast cytoplasm occurs in which the cytoplasm, associated with the degenerate nucleus, grows around the portion associated with the future spore nucleus. Continuity is believed to be maintained between the two portions of cytoplasm until later in spore maturation when complete cleavage occurs. They further suggested that the basic mechanism of sporoplasm delimitation may also occur in species of *Minchinia*. Such a mechanism could occur in *Minchinia* sp. following syncytium formation, but the evidence is inconclusive. It is true that developing spores are observed in which cup-shaped units of anucleate cytoplasm partially surround an uninucleate sporoplasm primordium; however, no cytoplasmic bridge was observed between the two and no degenerate nucleus was observed. Possibly cleavage of uninucleate sporoblasts occurs to yield the "cup" of cytoplasm and the sporoplasm as two distinct units followed by growth of the "cup" rim around the sporoplasm. Discontinuity between sporoplasm and extrasporoplasm cytoplasm is not difficult to accept early in spore morphogenesis, because it is well established that anucleate cells can carry on biosynthesis of macromolecules (Keck, 1969), thus synthesis of spore wall ornaments could possibly occur in anucleated cytoplasm of *Minchinia* sp. In addition, the sporoplasms of ascospores are delimited from the surrounding cytoplasm prior to wall formation, although wall formation does occur on the plasmalemma not in the cytoplasm surrounding the sporoplasm (Beckett et al., 1968; Carroll, 1969).

My observations of *M. nelsoni*, *M. costalis*, *M.* sp., and *U. crescens* further indicate that complete cleavage of the sporont frequently occurs to yield approximately spherical, uninucleate sporoblasts with no connection to a unit of cytoplasm which could be differentiated as an "envelope primordium" (see for example Fig. 12, Perkins, 1969). These spherical sporoblasts could cleave to form an anucleate "envelope primordium" as hypothesized by Ormières et al. (1973), but I have not seen evidence of it. Obviously the question as to how spores are formed will not be settled by observations of sectioned material from non-synchronously dividing cells. Living material or sections of synchronous cells fixed at known time intervals must be examined. Unfortunately it appears that the techniques and media required for culture of these organisms are unknown.

As I suggested earlier (Perkins, 1971), haplosporosomes appear to be characteristic of species of *Minchinia* and *Urosporidium*. Ormières et al. (1973) found them in *U. jiroveci* and now they have been found in *Minchinia* sp. Their function is unknown. Possibly isolation and subsequent biochemical characterization can be accomplished, thereby yielding an indication of their function. The ornaments or strands around the mature spore of *Minchinia* sp. are also consistent with the observations of the other species in that the spores of each species have one or two types of wrappings. These structures differ enough so that they could be used to distinguish the spores of the various species studied thus far except possibly *U. crescens* and *U. jiroveci* which seem to have the same structures.

Other workers such as Granata (1914), Pixell-Goodrich (1915), and Farley (1967) have either suggested or stated that karyogamy and subsequent meiosis are involved in sporulation in species of *Minchinia* and *Haplosporidium*, their chief evidence being the observations of paired nuclei and large variations in nuclear size. This study adds to those findings the observation of synaptonemal-like complexes and polycomplex-like structures as possible indicators of meiosis in sporonts. In addition, nuclear size changes during spore formation have been more thoroughly quantitated.

The morphogenetic sequence which appears to occur during sporulation is summarized in Figure 32. Plasmodia increase in mass and numbers of nuclei and form a delimiting wall at which time they are termed sporonts. The possibility that these increases result from plasmogamy of several plasmodia was not eliminated. Nuclear pairing follows, then karyogamy to form a brief diplophase in the life cycle, at which point nuclear sizes increase to about 4-6 μm diameter from about 2-4 μm. Meiosis results in reduction in nuclear size and a return to haplophase. The sporont then undergoes cytokinesis by one of two mechanisms. In one, the cytoplasm passes through a syncytial stage before grouping around nuclei to form uninucleate sporoblasts from which the sporoplasm is cleaved. In the other, both sporoplasms and sporoblasts are cleaved from the sporont forming free sporoblasts within the sporont wall and sporoplasms bound in the remaining cytoplasm of the sporont until subsequent cleavage frees them as sporoblasts with precleaved sporoplasm (Fig. 17). The latter mechanism is considered to be aberrant, because a large number of anomalously-formed spores are found in such sporonts; however, since spores, normal in appearance, are also observed and since the "aberrant" sporonts are frequently observed, they are believed to be a source of normal spores.

Since the proposed developmental sequence in Figure 32 is based on observations of non-living material, there are obviously many uncertainties concerning its accuracy. The evidence that karyogamy occurs during sporont de-

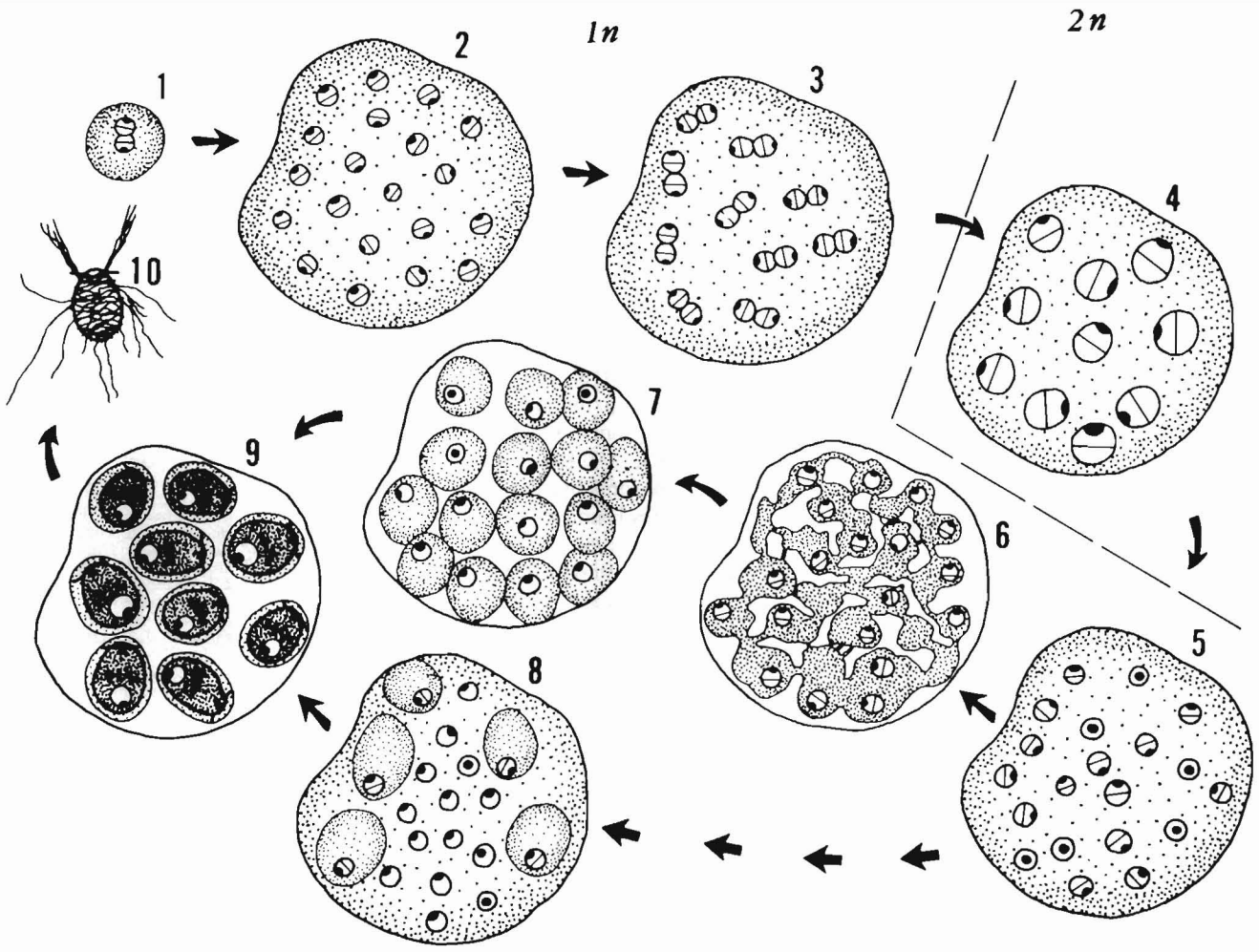

Figure 32.—Diagram of postulated sporulation sequence. Plasmodia (1) enlarge to form sporonts (2) (whether plasmogamy occurs is unknown) in which nuclei pair (3) then karyogamy results (4). The cells, therefore, pass from haplophase (1n) to diplophase (2n). Meiosis results in the return to haplophase and decrease in nuclear size (5). Cytokinesis occurs by one of two routes. In one a syncytium (6) is formed followed by condensation of cytoplasm around each nucleus to form uninucleate sporoblasts (7). In the other less significant pathway, sporoblasts or sporoplasms are cleaved from the sporont protoplast (8). Within sporoblasts cleavage occurs to yield sporoplasm surrounded by anucleate cytoplasm then a spore wall is formed at the interface of the two units (9) followed by spore maturation (10). Sporoplasms cleaved from the sporont protoplasm (8) are further delimited by cleavage of a unit of cytoplasm which surrounds them resulting in cells as seen in (9). The bars in nuclei represent the persistent mitotic apparatus.

velopment lies in the following observations: 1) a wide range of nuclear sizes (2.3-5.9 μm diameter) were observed in sporonts; 2) the larger nuclei were not the vesicular type thus are probably not the result of poor fixation as may be the case in plasmodia; 3) a pair of small nuclei (2.5 and 2.9 μm) were observed in a sporont with large nuclei (4.1-4.6 μm) (Fig. 9); 4) large (4-5.9 μm) nuclei were not paired.

Since large nuclei up to 8.0 μm were observed in plasmodia, there is a possibility that: 1) karyogamy occurs in plasmodia; 2) enlargement occurs before nuclear division; 3) there are two sexual strains with different size nuclei; or 4) enlargement is a fixation artifact. Either suggestions 1) or 3) could be correct, but there is not enough information to evaluate them at present. It is unlikely that marked nuclear enlargement is required before nuclear division in plasmodia, because anaphase and telophase division figures of different sizes were observed which correspond to the different sizes of interphase nuclei. The largest anaphase figure observed was 9.9 μm long $\times$ 5.1 μm wide and the smallest was 6.5 $\times$ 3.0 μm (N = 9). It is possible that enlargement could be the result of inadequate fixation, but this suggestion was not tested. Enlarged, vesicular nuclei have been noted by Haskin et al. (1966), Myhre (1969), and myself[3] in *M. nelsoni* plasmodia. As Myhre (1969) noted the large nuclei are "vesicular" with large unstained areas or spaces in the nucleoplasm. He noted also that nearly a full range of nuclei (2.0-7.5 μm) could be "vesicular," observations that I have verified for plasmodia of both *M. nelsoni* and *Minchinia* sp. After observations of thousands of *M. nelsoni* and hundreds of *Minchinia* sp. plasmodial nuclei fixed in glutaraldehyde and osmium tetroxide I have not seen the enlarged "vesicu-

[3]Perkins, Frank O. Fine structure of the haplosporidan *Kernstab*, a persistent, intranuclear mitotic apparatus. In preparation.

lar" nuclei. Only in material fixed in Davidson's, formol-alcohol, or Zenker's fixative were these nuclei seen. Small (<3.0 μm) vesicular nuclei were seen in the preparations for electron microscopy, but they were in moribund cells or associated with lysing oyster cells. Obviously, the matter of enlarged nuclei requires further examination.

As seen in Figure 10, attempts to clearly demonstrate two or three nuclear size classes were unsuccessful, possibly because of the inability to distinguish cell stages 2-5 (Fig. 32) (assuming that they exist). One would expect to see at least two modes if the small prekaryogamy (cell 2; Fig. 32) and post-meiotic (cell 5) nuclei were the same size and the post-karyogamy, large nuclei (cell 4) were in a different size range. A trimodal distribution would be expected if cells 2, 4, and 5 contained nuclei of different sizes. However, only a skewed distribution with one obvious mode was determined.

The evidence for meiosis lies in the observation of structures presumed to be synaptonemal complexes (SC's) and polycomplexes (PC's) (Figs. 11-13). Structures like those in Figures 11 and 12 are believed to be SC's because: 1) the structure and sizes are similar to SC's as previously described in other organisms (Perkins and Amon, 1969; Moens and Perkins, 1969; Wettstein and Sotelo, 1971); 2) they were found only in sporonts and were infrequently observed; 3) they were not present in paired nuclei; and 4) they were absent from nuclei, obviously in anaphase or telophase, as evidenced by nuclear membrane profiles. The chief difference between the present complexes and PC's reported from other organisms, such as the water mold *Lagenidium callinectes* (Amerson and Bland, 1973) or the mosquito *Aedes aegypti* (Roth, 1966), is the absence of medial elements in *Minchinia* sp. complexes. If the structures are PC's, possibly they represent degenerate forms in which the medial elements were lost or not preserved during fixation. Some PC-like structures in *Minichinia* sp. more closely resembled those of *L. callinectes* in that the dense bands were slightly bent in a shallow V-shaped or curved configuration.

I suggest that meiosis occurs in a nearly synchronous manner within each sporont (Fig. 14) to yield sporonts with nuclei of a size approximating those of prekaryogamy sporonts and those just before meiosis (Fig. 15). It was possible to identify late sporonts by the presence of incomplete cytoplasmic cleavage furrows. It is unlikely that cleaving plasmodia were misidentified as sporonts, because 1) plasmodia are much smaller and have fewer nuclei, 2) the sporont wall was visible on the cleaving cells, and 3) plasmodia were not observed to subdivide into uninucleate cells.

ACKNOWLEDGMENTS

I thank Marti Lewis, Carolyn Kerr and Diane Stallard for their able technical assistance and Norimitsu Watabe for providing the scanning electron micrograph. Joseph Gilley is thanked for preparation of the life cycle drawing and graphs.

LITERATURE CITED

Amerson, H. V., and C. E. Bland. 1973. The occurrence of polycomplexes in the nucleus of encysting spores of *Lagenidium callinectes*, a marine Phycomycete. Mycologia 65:966-970.

Andrews, J. D. 1966. Oyster mortality studies in Virginia. V. Epizootiology of MSX, a protistan pathogen of oysters. Ecology 47:19-31.

Beckett, A., R. Barton, and I. M. Wilson. 1968. Fine structure of the wall and appendage formation in ascospores of *Podospora anserina*. J. Gen. Microbiol. 53:89-94.

Carroll, G. C. 1969. A study of the fine structure of ascosporogenesis in *Saccobolus kerverni*. Arch. Mikrobiol. 66:321-339.

Couch, J. A. 1967. Concurrent haplosporidian infections of the oyster, *Crassostrea virginica* (Gmelin). J. Parasitol. 53:248-253.

Farley, C. A. 1967. A proposed life cycle of *Minchinia nelsoni* (Haplosporida, Haplosporidiidae) in the American oyster *Crassostrea virginica*. J. Protozool. 14:616-625.

Granata, L. 1914. Ricerche sul ciclo evolutivo di *Haplosporidium limnodrili* Granata. Arch. Protistenkd. 35:47-79.

Haskin, H. H., L. A. Stauber, and J. A. Mackin. 1966. *Minchinia nelsoni* n. sp. (Haplosporida, Haplosporidiidae): Causative agent of the Delaware Bay oyster epizoötic. Science (Wash., D.C.) 153:1414-1416.

Keck, K. 1969. Metabolism of enucleated cells. *In*: G. H. Bourne and J. F. Daniellai (editors), Int. Rev. Cytol. 26:191-233. Academic Press, N.Y.

Moens, P., and F. O. Perkins. 1969. Chromosome number of a small protist: Accurate determination. Science (Wash., D.C.) 166:1289-1291.

Myhre, J. L. 1969. Nucleic acid and nucleic protein patterns in vegetative stages of the haplosporidan oyster parasite, *Minchinia nelsoni* Haskin, Stauber and Mackin. Proc. Natl. Shellfish. Assoc. 59:52-59.

Ormières, R., and P. de Puytorac. 1968. Ultrastructure des spores de l'Haplosporidie *Haplosporidium ascidiarum* endoparasite die Tunicier *Sydnium elegans* Giard. C. R. Hebd. Seances Acad. Sci. Ser. D Sci. Nat. (Paris) 266:1134-1136.

Ormières, R., V. Sprague, and P. Bartoli. 1973. Light and electron microscope study of a new species of *Urosporidium* (*Haplosporida*), hyperparasite of trematode sporocysts in the clam *Abra ovata*. J. Invertebr. Pathol. 21:71-86.

Perkins, F. O. 1968. Fine structure of the oyster pathogen *Minchinia nelsoni* (Haplosporida, Haplosporidiidae). J. Invertebr. Pathol. 10:287-305.

———. 1969. Electron microscope studies of sporulation in the oyster pathogen, *Minchinia costalis* (Sporozoa: Haplosporida). J. Parasitol. 55:897-920.

———. 1971. Sporulation in the trematode hyperparasite *Urosporidium crescens* de Turk, 1970 (Haplosporida: Haplosporidiidae) - an electron microscope study. J. Parasitol. 57:9-23.

Perkins, F. O., and J. P. Amon. 1969. Zoosporulation in *Labyrinthula* sp.; an electron microscope study. J. Protozool. 16:235-257.

Pixell-Goodrich, H. L. M. 1915. *Minchinia*: A Haplosporidian. J. Zool. Lond. 1915:445-457.

Rosenfield, A., L. Buchanan, and G. B. Chapman. 1969. Comparison of the fine structure of spores of three species of *Minchinia* (Haplosporida, Haplosporidiidae). J. Parasitol. 55:921-941.

Roth, T. F. 1966. Changes in the synaptinemal complex during meiotic prophase in mosquito oocytes. Protoplasma 61:346-386.

Shaw, B. L., and H. I. Battle. 1957. The gross and microscopic anatomy of the digestive tract of the oyster *Crassostrea virginica* (Gmelin). Can. J. Zool. 35:325-347.

Sprague, V. 1963. *Minchinia louisiana* n. sp. (Haplospridia, Haplosporidiidae), a parasite of *Panopeus herbstii*. J. Protozool. 10:267-274.

Wettstein, R., and J. R. Sotelo. 1971. The molecular architecture of synaptonemal complexes. *In*: E. J. DuPraw (editor), Advances in cell and molecular biology. Vol. 1, p. 109-152. Academic Press, N.Y.

Wood, J. L., and J. D. Andrews. 1962. *Haplosporidium costale* (Sporozoa) associated with a disease of Virginia oysters. Science (Wash., D.C.) 136:710-711.

MFR Paper 1147. From Marine Fisheries Review, *Vol. 37, Nos. 5-6, May-June 1975. Copies of this paper, in limited numbers, are available from D83, Technical Information Division, Environmental Science Information Center, NOAA, Washington, DC 20235. Copies of* Marine Fisheries Review *are available from the Superintendent of Documents, U.S. Government Printing Office, Washington, DC 20402 for $1.10 each.*